5′TRU: Identification and Analysis of Translationally Regulative 5′Untranslated Regions in Amino Acid Starved Yeast Cells*[S]

Nicole Rachfall‡, Isabelle Heinemeyer§, Burkhard Morgenstern§, Oliver Valerius‡¶, and Gerhard H. Braus‡¶

We describe a method to identify and analyze *t*ranslationally *r*egulative 5′*U*TRs (5′TRU) in *Saccharomyces cerevisiae*. Two-dimensional analyses of ^{35}S-methionine metabolically labeled cells revealed 13 genes and proteins, whose protein biosynthesis is post-transcriptionally up-regulated on amino acid starvation. The 5′UTRs of the respective mRNAs were further investigated. A plasmid-based reporter-testing system was developed to analyze their capability to influence translation dependent on amino acid availability. Most of the 13 candidate 5′UTRs are able to enhance translation independently of amino acids. Two 5′UTRs generally repressed translation, and the 5′UTRs of *ENO1*, *FBA1,* and *TPI1* specifically up-regulated translation when cells were starved for amino acids. The *TPI1*-5′UTR exhibited the strongest effect in the testing system, which is consistent with elevated Tpi1p-levels in amino acid starved cells. Bioinformatical analyses support that an unstructured A-rich 5′ leader is beneficial for efficient translation when amino acids are scarce. Accordingly, the *TPI1*-5′UTR was shown to contain an A-rich tract in proximity to the mRNA-initiation codon, required for its amino acid dependent regulatory function. ***Molecular & Cellular Proteomics 10: 10.1074/mcp.M110.003350, 1–11, 2011.***

Gene expression is efficiently controlled by several regulatory mechanisms of protein biogenesis to adapt to changing endogenous and environmental conditions (1). Translational regulation has particular significance because it enables a quick and reversible adaptation, especially needed for efficient stress response (2). Stresses often induce *global control* mechanisms leading to the reduction of overall protein biosynthesis. This is mediated by post-translational modifications of one or more translation initiation factors (eIFs) including phosphorylations or changes in their abundance (1, 3). A well-studied example is the response to amino acid (aa)[1] starvation conditions. A lack of amino acids leads to increased phosphorylation of eIF2 and results in reduced formation of ternary complex (eIF2-GTP-Met-tRNA$_i^{Met}$) needed for translation initiation (4). This *global control* can be overruled by *mRNA-specific control* mechanisms to ensure efficient translation of specific mRNAs even when overall protein biosynthesis is reduced. Those mechanisms are especially directed by elements in the 5′ untranslated regions (5′UTRs) of mRNAs (1).

The paradigm of an mRNA more efficiently translated under aa-starvation conditions encodes Gcn4p, the global regulator of amino acid biosynthesis (5). This effect is mediated by four short upstream open reading frames in the 5′UTR of the *GCN4*-mRNA, repressing its translation under non-starvation conditions and derepressing it when amino acids are scarce (6). This regulative mechanism is conserved from yeast to the mammalian Gcn4p-homolog *a*ctivating *t*ranscription *f*actor 4 (ATF4), whose mRNA carries two upstream open reading frames in its 5′UTR (7, 8). Another feature known to regulate translation efficiency in yeast and human is the presence of internal ribosome entry sites (IRES) in the 5′UTR of mRNAs. They enable sufficient translation for specific mRNAs under conditions when canonical cap-dependent translation is inhibited by directly recruiting the ribosome to the vicinity of the initiation codon, thus bypassing the cap-structure and its associated eIFs (2). A necessity for cap-independent translation via IRES has been shown for starvation-induced differentiation in yeast. In contrast to the structure-based viral IRES-activity the activation in yeast is mediated by unstructured A-rich elements via recruitment of the poly(A) binding protein (Pab1p) (9). In accordance, strong IRES have recently been shown to possess weak secondary structures and to be predominantly located immediately upstream of the mRNA-initiation codon (10). The formation of stronger secondary structures on the other hand can influence translation efficiency via hairpin structures, inhibiting scanning of

From the ‡Institute of Microbiology and Genetics, Department of Molecular Microbiology and Genetics, §Department of Bioinformatics, Georg-August Universität, D-37077 Göttingen, Germany

Received July 18, 2010, and in revised form, March 7, 2011
Published, MCP Papers in Press, March 28, 2011, DOI 10.1074/mcp.M110.003350

[1] The abbreviations used are: 3AT, 3-amino-1,2,4-triazole; 5′TRU, translationally regulative 5′UTR; 5′UTR, 5′ untranslated region; aa, amino acid; eIF, eukaryotic translation initiation factor; IRES, internal ribosome entry site; MFE, minimal free energy.

TABLE I
Plasmids used in this work

Plasmid	Description	Reference
YEp355	7.94 kb vector, *amp^R (bla)*, *lacZ*, *ori, 2 μm, URA3*	ATCC, The Global Bioresource Center™ (Wesel, Germany)
pME3680	YEp355 containing ^{prom}*PGK1* followed by *Bam*HI restriction site and ATG start codon (testing vector)	This work
pME3681	pME3680 with *GCN4*-5′UTR introduced between ^{prom}*PGK1* and ATG start codon	This work
pME3682	pME3680 with *PGK1*-5′UTR introduced between ^{prom}*PGK1* and ATG start codon	This work
pME3683	pME3680 with *ASC1*-5′UTR introduced between ^{prom}*PGK1* and ATG start codon	This work
pME3684	pME3680 with *GRX1*-5′UTR introduced between ^{prom}*PGK1* and ATG start codon	This work
pME3685	pME3680 with *ENO1*-5′UTR introduced between ^{prom}*PGK1* and ATG start codon	This work
pME3686	pME3680 with *TRP5*-5′UTR introduced between ^{prom}*PGK1* and ATG start codon	This work
pME3687	pME3680 with *ILV5*-5′UTR introduced between ^{prom}*PGK1* and ATG start codon	This work
pME3688	pME3680 with *IPP1*-5′UTR introduced between ^{prom}*PGK1* and ATG start codon	This work
pME3689	pME3680 with *FBA1*-5′UTR introduced between ^{prom}*PGK1* and ATG start codon	This work
pME3690	pME3680 with *RHR2*-5′UTR introduced between ^{prom}*PGK1* and ATG start codon	This work
pME3691	pME3680 with *AHP1*-5′UTR introduced between ^{prom}*PGK1* and ATG start codon	This work
pME3692	pME3680 with *ALD6*-5′UTR introduced between ^{prom}*PGK1* and ATG start codon	This work
pME3693	pME3680 with *FPR1*-5′UTR introduced between ^{prom}*PGK1* and ATG start codon	This work
pME3694	pME3680 with *TPI1*-5′UTR introduced between ^{prom}*PGK1* and ATG start codon	This work
pME3783	pME3680 with *stem loop*-5′UTR introduced between ^{prom}*PGK1* and ATG start codon	This work
pME3784	pME3680 with Δ *last 25nt*-5′UTR introduced between ^{prom}*PGK1* and ATG start codon	This work
pME3785	pME3680 with *TPI1-Tp*-5′UTR introduced between ^{prom}*PGK1* and ATG start codon	This work
pME3786	pME3680 with *TPI1-Tc*-5′UTR introduced between ^{prom}*PGK1* and ATG start codon	This work
pME3787	pME3680 with *TPI1-Cp*-5′UTR introduced between ^{prom}*PGK1* and ATG start codon	This work
pME3788	pME3680 with *TPI1-Cc*-5′UTR introduced between ^{prom}*PGK1* and ATG start codon	This work
pME3789	pME3680 with *TPI1-Gp*-5′UTR introduced between ^{prom}*PGK1* and ATG start codon	This work
pME3790	pME3680 with *TPI1-Gc*-5′UTR introduced between ^{prom}*PGK1* and ATG start codon	This work
pME3791	pME3680 with *AHP1-A*-5′UTR introduced between ^{prom}*PGK1* and ATG start codon	This work

the 43S pre-initiation complex or binding of regulative proteins (1, 3).

Currently, there is only a small group of proteins for which a translational regulation has been described. Smirnova and colleagues performed polysome and microarray analyses to identify mRNAs that are translationally maintained after aa-depletion (11). These data represent a genome-wide approach for detecting potential candidates that are translationally regulated. Here, we describe a proteome-based approach to identify 5′UTRs regulating translation in dependence of aa-availability. Bioinformatical analyses of respective 5′UTRs disclosed a noticeable accumulation of adenine bases and their predicted secondary structures to be specifically weak or not present. The introduction of the 5′UTR sequences in a reporter-testing vector revealed three 5′UTRs that significantly increased translation when aa-starvation was induced. The strongest effects could be monitored for the unstructured *TPI1*-5′UTR. An A-rich tract in proximity to the AUG start codon was shown to be essential for the translationally regulative function of the *TPI1*-5′UTR in response to aa-starvation conditions.

EXPERIMENTAL PROCEDURES

Yeast Strains and Growth Conditions—The *Saccharomyces cerevisiae* strain RH2817 is of the Σ1278b background (*MATα*, *ura3–52*, *trp1::hisG*) (12). RH3384 and RH3385 were generated by C-terminally tagging *ENO1* and *FBA1* with 3xmyc, respectively, according to Janke and colleagues (13). Transformations were carried out according to the lithium acetate method (14). Cultures were grown at 30 °C overnight in 10 ml liquid minimal medium (YNB) containing respective supplements (amino acids, uracil), diluted and cultivated in main cultures to midlog phase before isolation of protein extracts or total RNA. Experiment-specific growth conditions are given in the respective paragraphs.

Plasmid Construction—All plasmids used in this study are listed in Table I. The *PGK1*-promoter was amplified with the primers 5′-GAT-*AGATCT*GCACGTGGCCTCTTATCGAG-3′ and 3′-CGAAAGAAAAA-GAGAAAAAATGTCTAGTAGTTCCTTC*GGATCC***ATG**TGG*AGATCT*T-C-5′ to construct the plasmid pME3680 (testing vector). This resulted in the *PGK1*-promoter fragment flanked by *Bgl*II restriction sites including a *Bam*HI restriction site and ATG start codon downstream of the promoter. The *Bgl*II restriction sites enable the introduction of the *PGK1*-promoter fragment into *Bam*HI restricted YEp355. To construct plasmids ‘pME3681 - pME3694′ and ‘pME3783 - pME3791 respective 5′UTRs were amplified by PCR, inserting *Bgl*II restriction sites on both ends, and ligated with pME3680 using the *Bam*HI restriction site previously introduced by PCR. 5′UTR-lengths were determined according to David and colleagues (15) (www.ebi.ac.uk/huber-srv/queryGene, Table II) and sequences were confirmed by sequencing (see supplemental Table S1 and Fig. 5*A*). Plasmids were propagated in the *Escherichia coli* strain DH5α in LB medium with 100 μg/ml ampicillin.

De Novo Proteome and Two-dimensional-PAGE Analysis—Amino acid starvation conditions were induced by the histidine analog 3-amino-1,2,4-triazole (3AT). 50 ml yeast cultures were grown to midlog phase (OD_{600} = 0.8) in minimal medium prior to the addition of 3AT to a final concentration of 10 mM (16) and further incubated for 30 min at 30 °C. Then 450μCi Met-[^{35}S]-label (Hartmann Analytik, Braun-

TABLE II

Core information of bioinformatical 5′UTR-analysis. For every analyzed 5′UTR sequence its minimal free energies (MFEs) were determined by RNALFOLD (see supplemental Table S4) and the respective greatest negative MFE (minMFE) listed here. Start point and length of the corresponding secondary structure predicted are denoted with position one matching the first nucleotide of the respective 5′UTR at its 5′end. The GC- and A-content for each 5′UTR sequence are given in percentage. An increase in A-content of at least 20% within the last 25 nt of the 5′UTR is indicated by asterisks

mRNA	length of 5′UTR [nt]	minMFE [kcal/mol]	start of structure	length of structure [nt]	GC-content [%]	A-content [%]	A-content last 25nt [%]
AHP1	49	-	-	-	35	53	52
ALD6	65	-0.63	1	42	26	52	52
ASC1	34	-1.9	11	21	24	53	60
ENO1	38	-	-	-	34	50	60*
FBA1	56	-	-	-	25	32	52*
FPR1	31	-	-	-	19	65	68
GRX1	68	-6.3	4	59	34	44	64*
ILV5	91	-7.9	17	44	26	47	64*
IPP1	59	-6.4	1	39	41	24	24
PGK1	82	-9.7	1	63	23	34	52*
RHR2	53	-1.5	4	24	24	46	56*
TPI1	45	-	-	-	22	53	68*
TRP5	47	-5.2	8	35	47	38	40

schweig, Germany) were added and the cultures incubated for an additional hour. Cells were harvested and washed in wash buffer (0.1 M Tris, pH 8.0 with 1% DMSO and 1 mM PMSF). Protein extracts were obtained by lysing cells with Y-PER® Plus reagent (#78999, Pierce, Rockford, IL), containing Complete Protease Inhibitor Cocktail (Roche Diagnostics GmbH, Mannheim, Germany) and purification by methanol-chloroform extraction (17). Protein concentrations were determined via BCA Protein Assay kit from Pierce (#23227). One hundred micrograms of purified protein extracts were used in two-dimensional-PAGE analyses. For the first dimension the protein samples were applied to Immobiline Drystrips (pH 4–7, 18 cm, #17–1233-01, GE Healthcare Europe GmbH, Freiburg, Germany) via rehydration loading. The separation was carried out in the Ettan IPGphor Isoelectric focusing system (GE Healthcare) at 20 °C and a maximum of 50μA/strip with the following program: 70 V for 12 h (step-n-hold), 500V for 1h (step-n-hold), 1000V for 1h (step-n-hold), 8000V for 1h (gradient), 8000V for 4 h (step-n-hold). The strips were thereafter equilibrated in equilibration buffer (50 mM Tris-HCl, pH 8.8, 6 M urea, 30% (v/v) glycerol, 2% (w/v) SDS, 0.002% BPB) containing 325 μl 1 M dithiotreitol (DTT) or 125 mg iodacetamide and incubated for 30 min, respectively. The second dimension separation was executed on 12.5% polyacrylamide gels in Protean® II xi vertical electrophoresis cells (1 mm spacers, 20 × 20 cm glass plates) (Bio-Rad Laboratories GmbH, Munich, Germany). Electrophoresis was performed at 30 mA per gel. Gels were silver-stained according to Blum *et al.* (18), vacuum dried, and exposed on imaging plates (Fuji, Tokyo, Japan) for two weeks. The protein-spots in the resulting autoradiographies were quantified with the analysis software PDQuest™ (Bio-Rad, Munich, Germany). The analysis was performed for five biologically independent replicates.

LC-MS/MS Protein Identification—Excised polyacrylamide gel pieces of stained protein-spots were digested with trypsin according to Shevchenko *et al.* (19). Tryptic peptides extracted from each gel piece were injected onto a reverse-phase liquid chromatographic column (Dionex-NAN75–15-03-C18 PM) using the *ultimate* HPLC system (Dionex, Idstein, Germany) to further reduce sample complexity prior to mass analyses with an LCQ DecaXP mass spectrometer (Thermo Scientific, San Jose, CA), equipped with a nano-electrospray ion source. Cycles of MS spectra with *m/z* ratios of peptides and four data-dependent MS2 spectra were recorded by mass spectrometry. The "peak list" was created with *extractms* provided by the Xcalibur software package (BioworksBrowser 3.3.1, Thermo Scientific). The MS2 spectra with a total ion current higher than 10.000 were used to search for matches against a yeast genome protein sequence database from the National Center for Biotechnology Information (NCBI) *Saccharomyces Genome Database* (Stanford, CA, USA, 6882 sequences, March 2005, plus 180 sequences of the most commonly appearing contaminants as *e.g.* keratins and proteases, provided with the BioworksBrowser package) using the TurboSEQUEST algorithm (20) of the Bioworks software. The search parameters based on the TurboSEQUEST software included: (i) precursor ion mass tolerance less than 1.4 amu, (ii) fragment ion mass tolerance less than 1.0 amu, (iii) up to three missed tryptic cleavages allowed, and (iv) fixed cysteine modifications by carboxyamidomethylation (plus 57.05 amu) and variable modifications by methionine oxidation (plus 15.99 amu), and phosphorylation of serine, threonine, or tyrosine (plus 79.97 amu). At least two matched peptide sequences of identified proteins must pass the following criteria: (i) the cross-correlation scores (XCorr) of matches must be greater than 2.0, 2.5, or 3.0 for peptide ions of charge state 1, 2, and 3, respectively, (ii) ΔCn values of the best peptide matches must be at least 0.4, and (iii) the primary scores (Sp) were at least 600. Peptides of identified proteins were individually blasted against the SGD database (BLASTP at http://seq.yeastgenome.org/cgi-bin/blast-sgd.pl against the data set *Protein Encoding Genes*) to ensure their unambiguous assignment to the TurboSEQUEST-specified protein.

β-Galactosidase Assay—Assays were performed with extracts of cells grown in liquid minimal medium. 10 ml precultures were grown overnight at 30 °C and 1 ml used to inoculate 10 ml main cultures. For non-starvation conditions cells were harvested after 6 h. To induce amino acid starvation conditions, 3AT was added to a final concentration of 10 mM and cells were incubated at 30 °C for 8 h to compensate for a reduced growth rate under aa-starvation conditions. Specific β-galactosidase activities were normalized to the total protein amount (21) in each extract and calculated according to Rose and Botstein (22) (A_{415} × 0.3)/(0.0045 × protein concentration × extract volume × time).

Western Hybridization Analysis—Cell main cultures were grown in 50 ml minimal media at 30 °C to midlog phase (OD_{600} = 0.8) before further incubation with or without 10 mM 3AT for 1.5 h. Protein extraction was performed as previously described for the two-dimensional-PAGE analysis and proteins were blotted onto nitrocellulose

membrane subsequently of separation by one-dimensional or two-dimensional PAGE. After incubation of membranes with polyclonal rabbit anti-eIF2α-P (BIOSOURCE, Nivelles, Belgium), polyclonal rabbit anti-eIF2α, rabbit anti-Tpi1, monoclonal mouse anti-myc (#sc-40, Santa Cruz Biotechnology, Heidelberg, Germany) or polyclonal rabbit anti-Cdc28 (#sc-28550) antibodies and subsequent incubation with polyclonal peroxidase-coupled goat anti-mouse (#115–035-003, Dianova, Hamburg, Germany) or goat anti-rabbit (#G21234, MoBiTec, Göttingen, Germany) secondary antibodies, proteins were visualized by ECL technology (Amersham Biosciences, Munich, Germany). Relative quantification was carried out via PDQuest™ analysis software (Bio-Rad, Munich, Germany).

Northern Hybridization Analysis—Yeast cultures were cultivated according to the western hybridization protocol. Total RNA from yeast was isolated following the protocol described by Cross and Tinkelenberg (23). The RNA samples were denatured and separated on a 1.4% agarose gel containing 3% formaldehyde and transferred onto nylon membranes by capillary blotting. Gene specific probes were labeled radioactively with [α-^{32}P]dATP using the Prime-It® II Random Primer Labeling Kit from Stratagene (#300385, La Jolla, CA). A Fuji Film BAS-1500 Phosphor-Imaging scanner (Fuji, Tokyo, Japan) and Aida Image Analyzer software (Version 4.22.034, raytest, Straubenhardt, Germany) were used for quantification of signals.

Detection of Local, Thermodynamically Optimal RNA Secondary Structures—RNALFOLD from the VIENNA Package 1.8.2 (24) was used for the detection of local, thermodynamically optimal RNA secondary structures in 5′UTRs and the computation of their minimal free energy (MFE). The program was called with the options "-noLP" and "-L 100". The first option inhibits lonely base pairs and the second restrains the maximal local structure size to 100 bases.

Calculation of the z-Score—The z-score is computed for each subsequence in each 5′UTR with a local, thermodynamic optimal RNA secondary structure and is defined as: $z = (m - \mu) : \sigma$, whereby, m is the MFE of the secondary structure of the target sequence S, μ is the mean, and σ the standard deviation of the MFE-values of the RNA secondary structures of random sequences with the same length and dinucleotide composition as S. The creation of random sequences with similar properties as the target sequence is done by DISHUFFLE (25). For each target sequence 100 random sequences were computed. For each of the random sequences the secondary structure is predicted with RNAFOLD also from the VIENNA Package 1.8.2 (26). Then, for each target sequence the mean μ and standard deviation σ of the MFE-values of the random sequences and the z-score are computed.

RESULTS

In our analysis, we are aiming to find 5′UTRs that specifically enhance the translation of their respective mRNA under aa-starvation conditions induced by the histidine analog 3-amino-1,2,4-triazole (3AT). The strategy to identify regulatory 5′UTRs is based on (i) the two-dimensional-analysis of ^{35}S-methionine labeled *de novo* proteomes generated under differential conditions. The next steps of the analysis consist of (ii) identification of protein-spots regulated under the chosen condition, (iii) comparison of the obtained proteome data with pre-existing transcriptome data generated under similar conditions (27), (iv) evaluation of the candidate-5′UTRs via reporter-testing system presented in this study and (v) sequential and structural analysis of 5′UTRs by bioinformatical means (overview in supplemental Fig. S1).

The De Novo Biosynthesis of Various Abundant Proteins is Up-regulated Post-transcriptionally Upon Amino Acid Starvation—Wild type yeast cells of the Σ1278 background were cultivated in the absence or presence of 10 mM 3AT for 30 min. After the addition of ^{35}S-methionine the cultures were incubated for an additional hour. This enables the visualization of the effects of aa-starvation on *de novo* protein biosynthesis in *S. cerevisiae* via autoradiographies, opposing to a conventional steady-state proteome. The effective induction of aa-starvation conditions by 10 mM 3AT was verified at the level of translational regulation by a significant increase in eIF2-phosphorylation (supplemental Fig. S3A). The consequential reduction in overall protein biosynthesis and successful incorporation of radioactively labeled methionine during translation could be monitored for the soluble and insoluble fraction, resulting from cell lysis by Y-PER® Plus reagent, via scintillation counting (supplemental Fig. S3B). The radioactive labeling of proteins by ^{35}S-methionine during translation enables the generation of autoradiographies from two-dimensional gels (Fig. 1). In comparison to the silver-stained gels, the autoradiographies only illustrate proteins that were synthesized when aa-starvation conditions were already induced and depict changes in protein biosynthesis mediated by the addition of 3AT.

Our two-dimensional analysis was conducted on the basis of five biological replicates. It revealed a total number of 31 proteins, which showed an up-regulation under aa-starvation conditions (Fig. 2). The corresponding proteins can be assigned to several biological functions and take part in cellular processes like amino acid biosynthesis, glycolysis, oxidative stress response, and cell biogenesis. The fold changes ($^{+3AT}/_{-3AT}$) for the up-regulated protein-spots were determined by the analysis of the autoradiographies via PDQuest™ and range from 1.10 for Grx1p to 9.93 for Bna1p.

The obtained proteome data was compared with transcriptome data generated under similar conditions of non-starvation and aa-starvation (27) (10 mM 3AT, 8 h) (Fig. 2). For more than half of the candidates with elevated protein-spot intensities under aa-starvation conditions an up-regulation could also be found on their mRNA-level (Fig. 2, bottom part of chart). This comparison shows that the underlying regulation for these candidates is most likely to be found on the level of transcription even though an additional post-transcriptional regulation is not excluded. For the remaining 13 identified proteins a comparison of their proteome fold change with the fold change of their mRNA levels ($^{+3AT}/_{-3AT}$) revealed that a post-transcriptional regulation can be assumed. Their spot-intensities are elevated under aa-starvation conditions, whereas their corresponding mRNA levels either stay the same or are down-regulated when aa-starvation is induced (Fig. 2, top part of chart). Because of this discrepancy in the transcriptome and proteome changes, these candidates are of specific interest in this study and define the base for further investigations. A "confidence factor" is created as a means to

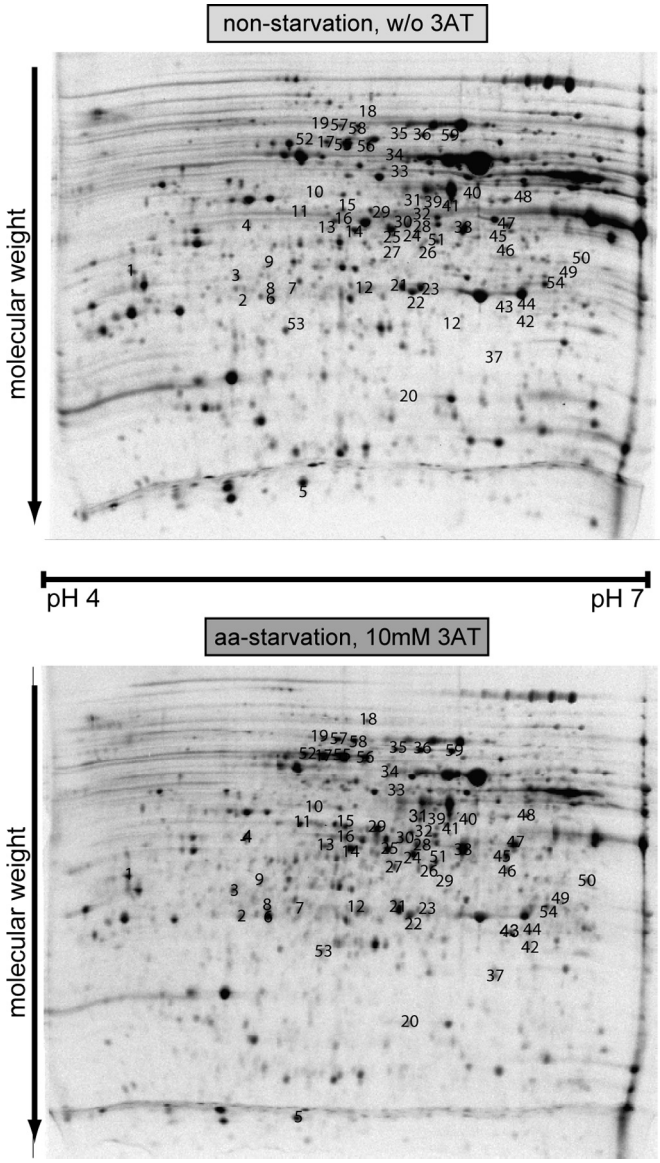

FIG. 1. **De novo proteome of the soluble cell fraction obtained under non-starvation (w/o 3AT) and aa-starvation (10 mM 3AT).** Autoradiographies corresponding to two-dimensional-PAGE (supplemental Fig. S2) of ^{35}S-methionine radioactively labeled proteins. The numbers indicate excised protein-spots with an enhanced intensity under aa-starvation conditions.

facilitate the assessment of a candidate's potential to be post-transcriptionally regulated. It factors in the determined *de novo* proteome changes under aa-starvation conditions in context with the transcriptome changes. Furthermore the number of autoradiographies in which a protein was found to be up-regulated is accounted for.

Novel Reporter-testing System to Monitor Translational Regulation Mediated by 5′UTRs—Translational control of individual mRNAs often depends upon the sequential characteristics and/or structural features of the transcript itself. Primarily 5′UTRs are known to contain a variety of elements with a regulatory effect on the translation of their mRNAs (1). This encouraged us to develop a straightforward *lacZ*-reporter-based testing system to enable the identification of 5′UTR sequences altering translation (Fig. 3*A*). Transcription consequently results in a *lacZ*-mRNA carrying the incorporated 5′UTR as its own. The practicability of this system to monitor translational regulation was verified by the incorporation of the 5′UTR of the *GCN4*-mRNA, known to alter translation efficiency in dependence of aa-availability (6) (supplemental Fig. S4).

The 5′UTRs to be analyzed via the testing system correspond to the 13 candidates post-transcriptionally up-regulated in their biosynthetic activity upon aa-starvation conditions (Fig. 2, top part, supplemental Table S2). For most of the 5′UTR sequences inserted in the reporter-testing vector (TV) an increase in β-galactosidase activity can be monitored under nonstarvation (-3AT) as well as under aa-starvation (+3AT) conditions. It reaches up to 16-fold relative to the empty TV, suggesting a general promotion of translation by the respective 5′UTRs (representative 5′UTR effects shown in Figs. 3*C* and 3*D*). However, two 5′UTRs investigated have the contrary effect on *lacZ*-mRNA expression (Fig. 3*B*). The insertions of the 5′UTRs of the *PGK1*- and *RHR2*-mRNA cause a distinct reduction of β-galactosidase activity compared with the empty TV. For the *RHR2*-5′UTR this effect is limited to aa-starvation. For the *PGK1*-5′UTR a drastic reduction in activity manifests under both conditions of aa-availability to as low as 30% of the empty TV-activity. A significant elevation in β-galactosidase activity from non-starvation to aa-starvation conditions could be monitored for three candidate-5′UTRs, namely *ENO1*-, *FBA1*- and *TPI1*-5′UTR, and ranges from 1.7 for the *ENO1*-5′UTR to 4.1 for the *TPI1*-5′UTR (Fig. 3*D*). This suggests a distinct role of those three 5′UTRs in enabling an enhanced translation of their respective mRNAs under aa-starvation conditions, when the translation of most mRNAs is reduced.

The mapping of the transcription start sites illustrates that within each construct one main transcription start sites is used under non-starvation as well as aa-starvation conditions and therefore identical mRNAs are entering translation under either aa-availability (supplemental Fig. S6). These findings argue for a translational regulation underlying the measured increase of β-galactosidase activity from non-starvation to aa-starvation for the 5′UTRs of *ENO1*, *FBA1,* and *TPI1*.

Correlation Between De Novo Biosynthesis and Total Protein Amount of Candidate Proteins Within the Cell—In this study we chose the method of metabolically labeling proteins by ^{35}S-methionine in the course of translation. The successive analysis of the respective autoradiographies discloses aa-dependent changes in the *de novo* protein biosynthesis in comparison to the steady-state total protein amount given at a certain time point. This represents a sensitive approach and enables the visualization of even subtle changes in the *de novo* biosynthesis for a specific protein. At this time point

FIG. 2. **Comparison of proteome and transcriptome data generated to monitor effects of aa-starvation conditions.** All candidates listed were found to be up-regulated upon aa-starvation in the proteome analyses (see supplemental Table S2 for corresponding protein names/functions and supplemental Table S3 for data on protein sequence identification). The transcriptome data used in this comparison has been obtained under similar conditions ([a27]). Transcriptome as well as proteome changes induced by aa-starvation conditions are displayed as the quotient of spot-intensity under aa-starvation to spot-intensity under non-starvation conditions ($^{+3AT}/_{-3AT}$). To clearly illustrate up- and down-regulation, transcriptome and proteome changes are visualized logarithmically in a horizontal histogram. The reproducibility for each candidate is expressed as frequency, describing the number by which a protein has been identified as up-regulated in *n* of five biological replicates. The last column represents the 'confidence factor' which is composed of the fold change ($^{+3AT}/_{-3AT}$) of the proteome relative to that of the transcriptome and the frequency of each proteome candidate.

candidate	transcriptome[a]		proteome		frequency	confidence factor
	$^{+3AT}/_{-3AT}$	$\log_{10}$	$^{+3AT}/_{-3AT}$		identifications in n of 5 autoradiographies	proteome/transcriptome x frequency
Cpc2/Asc1	0.76	-0.12 / 0.63	4.23		4	**22.3**
Tpi1	0.87	-0.06 / 0.58	3.76		4	**17.3**
Fba1	1.00	0 / 0.79	6.22		2	**12.4**
Ald6	0.77	-0.11 / 0.51	3.21		2	**8.3**
Ipp1	0.99	0 / 0.34	2.19		3	**6.6**
Rhr2	0.87	-0.06 / 0.65	4.47		1	**5.1**
Pgk1	0.60	-0.22 / 0.40	2.54		1	**4.2**
Fpr1	0.89	-0.05 / 0.53	3.37		1	**3.8**
Ilv5	0.93	-0.03 / 0.33	2.15		1	**2.3**
Trp5	0.83	-0.08 / 0.19	1.54		1	**1.9**
Ahp1	0.97	-0.01 / 0.23	1.70		1	**1.8**
Eno1	0.79	-0.10 / 0.10	1.25		1	**1.6**
Grx1	0.99	0 / 0.04	1.10		1	**1.1**
Rib5	1.23	0.1 / 0.65	4.48		5	**18.2**
Tdh3	1.24	0.09 / 0.62	4.21		5	**17.0**
Yhr029c	2.16	0.33 / 0.91	8.08		4	**15.0**
Bna1	2.08	0.32 / 1.0	9.93		3	**14.3**
Arg1	1.65	0.22 / 0.49	3.09		4	**7.5**
Ecm40	1.28	0.20 / 0.36	2.30		4	**7.2**
Aro8	1.45	0.16 / 0.53	3.39		3	**7.0**
Hor2	1.29	0.11 / 0.53	3.41		1	**5.3**
Thr1	1.43	0.16 / 0.33	2.13		3	**4.5**
Ccp1	1.72	0.24 / 0.29	1.96		3	**3.4**
Ubc13	1.13	0.05 / 0.25	1.79		2	**3.2**
His7	3.28	0.40 / 0.52	2.49		3	**2.3**
Sod2	1.22	0.11 / 0.37	2.34		1	**1.9**
Bmh2	1.13	0.05 / 0.26	1.83		1	**1.6**
Pdc1	1.04	0.02 / 0.17	1.47		1	**1.4**
His1	1.60	0.20 / 0.35	2.23		1	**1.4**
Ade1	2.04	0.31 / 0.45	2.80		1	**1.4**
Gcv3	1.83	0.26 / 0.37	2.37		1	**1.3**

changes in total protein amount within the cell might not yet be detectable. Eno1p, Fba1p, and Tpi1p were identified as proteins to be more efficiently synthesized under aa-starvation conditions (Fig. 4*A*). The analysis of the respective 5′UTRs via testing system further suggests an underlying 5′UTR-mediated translational regulation for these candidates (Fig. 3*D*). We questioned whether these translational changes might be strong enough to be reflected in elevated steady-state protein amounts of Eno1p, Fba1p, and Tpi1p after 90min of aa-starvation, whereas it is to mention that these candidates are proteins of high abundance. In the performed two-dimensional Western blot experiments several processed forms can be detected for all three proteins. All forms seem to underlie the same regulatory effect upon aa-starvation, according to their uniform change in abundance (Fig. 4*A*).

The determined steady-state protein amounts of myc-tagged Eno1p and Fba1p are not significantly increased under aa-starvation conditions. This suggests that the existing changes in their *de novo* protein biosynthesis are not extensive enough to effectively influence their steady-state protein amount after 90 min of treatment with 10 mM 3AT. Another possibility might be that the turnover rate for these proteins is more rapid under aa-starvation conditions than their increase in *de novo* biosynthesis. In contrast, for Tpi1p a significant increase in total protein could be determined even after only 90 min of growth under aa-starvation conditions. This implies a considerable enhancement in the translational rate of the *TPI1*-mRNA upon induction of starvation, quickly enlarging the pool of available Tpi1p in the cell. In the proteome analysis of radioactively labeled protein extracts Tpi1p was identified with an average up-regulation of 3.8 from non-starvation to aa-starvation conditions (Fig. 2). This is similar to the up-regulation of total Tpi1p amount in the cell with a factor of 3.3 determined via two-dimensional Western blot experiment (Fig. 4*A*). In addition, the measured effects from non-starvation to aa-starvation conditions in the β-galactosidase assays were the highest when the *TPI1*-5′UTR was inserted in the reporter-testing vector with a factor of 4.1 (Fig. 3*D*). The mRNA-levels of *ENO1*, *FBA1,* and *TPI1* are not significantly up-regulated when aa-starvation is induced and confirm the

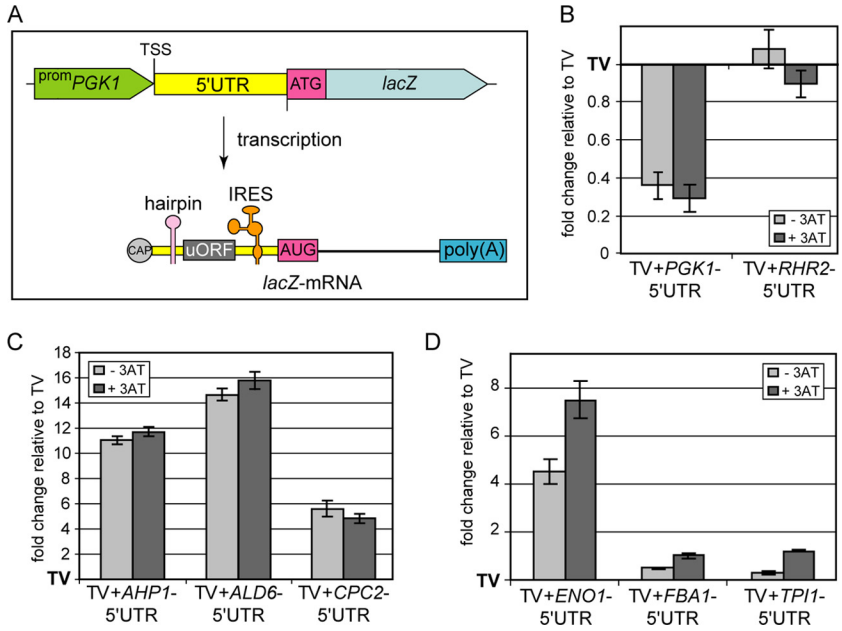

FIG. 3. **Reporter-testing system and β-galactosidase assays displaying the effects of candidate-5′UTRs on *lacZ*-reporter activity dependent on aa-availability.** *A*,The reporter-testing vector is a 2 μm yeast-*E. coli* shuttle vector carrying selectable marker genes as well as the constitutive *PGK1*-promoter with a defined transcription start site (TSS) and a *lacZ*-reporter-gene. Arbitrary 5′UTR sequences can be inserted in between promoter and reporter gene. Possible incorporated translationally regulative elements are depicted in the *lacZ*-mRNA-5′UTR such as hairpin structures, upstream open reading frames (uORFs) and internal ribosome entry sites (IRES). The three observed effects on *lacZ*-expression upon introduction of candidate 5′UTR sequences are illustrated in: *B*, reduced expression w/o significant 3AT effect; *C*, enhanced expression w/o significant 3AT effect; and *D*, enhanced expression w/additional positive 3AT effect. β-galactosidase activities were normalized to respective plasmid copy numbers (supplemental Fig. S5A) and are displayed relative to the testing vector without 5′UTR under the respective condition.

microarray data used in this study (Fig. 4*B*). Taken together these findings strongly suggest an aa-dependent translational regulation of Tpi1p biosynthesis mediated by elements in its 5′UTR. The resulting effects prove to be significant enough to affect the total Tpi1p amount in the cell even after a relatively short period of time.

Regulative 5′UTR Sequences are A-Rich and Weakly Folded—In addition to the experimental evaluation of the candidate-5′UTRs, they were analyzed bioinformatically. A first comparison of the respective 13 5′UTRs with each other revealed no distinct structural features or obvious consensus sequences. The lengths of the analyzed 5′UTR sequences are slightly shorter than the average length of 89 nucleotides (nt) determined for 5′UTRs in yeast. They rather agree with the majority of yeast-5′UTRs, measuring less than 50 nt in length (28) (Table II). This rather short length of most candidate-5′UTRs is regarded as indicator for a facilitated translation (28). Correspondingly, elevated *lacZ*-expressions were achieved by all but two of the thirteen 5′UTR sequences evaluated via reporter-testing system. To determine the potential and characteristics of secondary structure formation the minimal free energies (MFEs) for each 5′UTR sequence were predicted (supplemental Table S4). Hereby, the predicted structures are considered more stable the greater their negative free energies are. The greatest negative free energy (minMFE) found within each respective 5′UTR is listed in Table II along with the start and length of the corresponding secondary structure. The structures predicted stretch from 21 to 63 nt in length with an average of 41 nt. The corresponding average minMFE for the predicted secondary structures lies at −4.9 kcal/mol. The weakest MFE of −0.63 kcal/mol was predicted for the *ALD6*-5′UTR and the greatest for the *PGK1*-5′UTR at –9.7 kcal/mol. Even though the greatest minimal free energy was predicted for one of the longest 5′UTRs, belonging to the mRNA of *PGK1* (82 nt), there seems to be no obvious correlation between MFE gained from secondary structure formation and 5′UTR-length as far as this can be stated by this rather small group of 5′UTR sequences analyzed. No secondary structure was predicted for the 5′UTR sequences of *AHP1*, *ENO1*, *FBA1*, *FPR1,* and *TPI1* (Table II). Overall these findings imply a weak secondary structure formation for the candidate-5′UTRs. In addition, a comparison of the stabilities of the mRNA structures formed by the candidate 5′UTRs and randomly computed sequences of the same length and dinucleotide composition was performed. The resulting z-score further confirms the lack of significant secondary structure formation in the candidate-5′UTRs (supplemental Table S4). When evaluating the obtained structural information in combination with the data generated in the β-galactosidase assays, it is striking that for all 5′UTRs, showing an aa-dependent up-regulation of translation in the reporter-assays, namely *ENO1*-, *FBA1*-, and *TPI1*-5′UTR, no

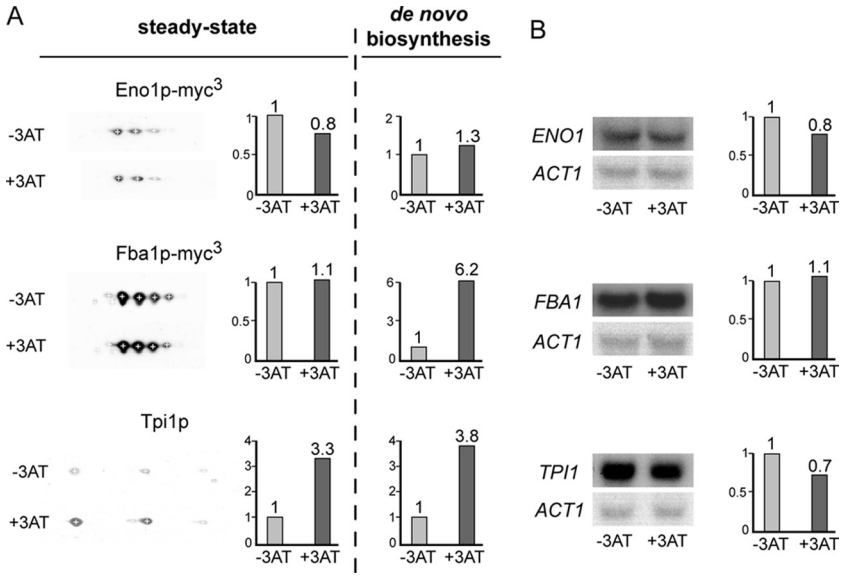

FIG. 4. **Steady-state protein- and mRNA-amount of candidates determined under non-starvation (-3AT) and aa-starvation (+3AT) conditions.** *A*, myc^3-tagged versions of the candidate-proteins Eno1p and Fba1p were hybridized to anti-myc antibody, whereas Tpi1p was detected by anti-Tpi1 antibody. For quantification the total intensity of all spots marked by crosshairs under the respective condition was determined. The illustrated change in *de novo* biosynthesis was previously determined by two-dimensional-PAGE of metabolically labeled protein extracts and autoradiography analysis (see Figs. 1 and 2). *B*, Northern hybridizations against *ENO1*-, *FBA1*- and *TPI1*-mRNA were quantified and normalized against *ACT1* as loading control. The adjacent graphs, respectively, illustrate the fold changes relative to the signal strengths under non-starvation conditions. Cells were grown to exponential phase before further incubation for 90 min in absence (-3AT) or presence (+3AT) of 10 mM 3AT.

secondary structure could be predicted. This was only the case for two other 5′UTRs in the bioinformatical analysis (Table II). Thus, the share of 5′UTRs without predicted secondary structure is well-above average for the group of 5′UTRs showing an aa-specific effect.

In addition to the MFEs, the GC-content for each 5′UTR sequence was determined averaging at 29% (Table II). Interestingly, this is consistent with the average GC-content found for the least stable structures in a genome-wide analysis of 5′UTRs in comparison to 47% for the most stable structures (29). Another striking feature is the high amount of adenine bases contained in the analyzed 5′UTR sequences. It even further increases to over 50% for all but two 5′UTRs proximal to the AUG translation initiation codon. For seven of the thirteen 5′UTR sequences this increase amounts to at least 20% including the 5′UTRs of *ENO1*, *FBA1,* and *TPI1* (Table II).

Because of the elevated *de novo* biosynthesis of Tpi1p and its increased protein levels under aa-starvation conditions, the 5′UTR of *TPI1* was analyzed in more detail. Several altered 5′UTRs were constructed and evaluated via reporter-testing system with special regard to the prominent A-rich tract in proximity to the AUG start codon, which leads to an adenine-content of 68% in the last 25 nt of the *TPI1*-5′UTR (Fig. 5*A*). The deletion of the last 25 nt of the *TPI1*-5′UTR, containing the A-rich tract, leads to a decreased β-galactosidase activity under non-starvation and aa-starvation conditions and clearly reduces the degree of activity gain in response to aa-starvation in comparison to the full length *TPI1*-5′UTR (Fig. 5*B*). The significance of the adenine bases within the Tpi1–5′UTR sequence was further examined by replacing the adenine bases with thymine, cytosine, or guanine bases, while still retaining the unstructured characteristic of the natural wild-type *TPI1*-5′UTR. The implications of a complete (c) loss of adenine bases in the *TPI1*-5′UTR were determined as well as of a partial (p) loss, limited to the last 25 nt containing the A-rich tract (Fig. 5).

The 5′UTR with a partial replacement of adenine with thymine bases (Tp) results in a complete loss of the aa-starvation-dependent up-regulation of β-galactosidase activity, characteristic for the wild type *TPI1*-5′UTR, whereas *lacZ*-expression under non-starvation conditions is not influenced (Fig. 5*B*). The complete substitution of all adenine bases with thymine also disables an elevated β-galactosidase activity under aa-starvation conditions and, in addition, reduces overall expression levels in comparison to the wild type *TPI1*-5′UTR and the *TPI1*-Tp exchange. Similarly, the complete or partial exchanges by cytosine or guanine bases do not significantly promote an induced *lacZ*-expression under aa-starvation but lead to a drastic reduction of β-galactosidase activity under both conditions. Hereby the complete replacement with cytosine bases and both guanine substitutions (Gp and Gc) resemble the total loss of β-galactosidase activity as measured for the introduction of a 52 bp stem loop structure with an MFE of −42.9 kcal/mol (30) (Fig. 5*B*).

As with the *TPI1*-5′UTR, the *AHP1*-5′UTR has no predicted secondary structure and displays a similar length but is distinguished by a clearly reduced A-content in its last 25 nt of

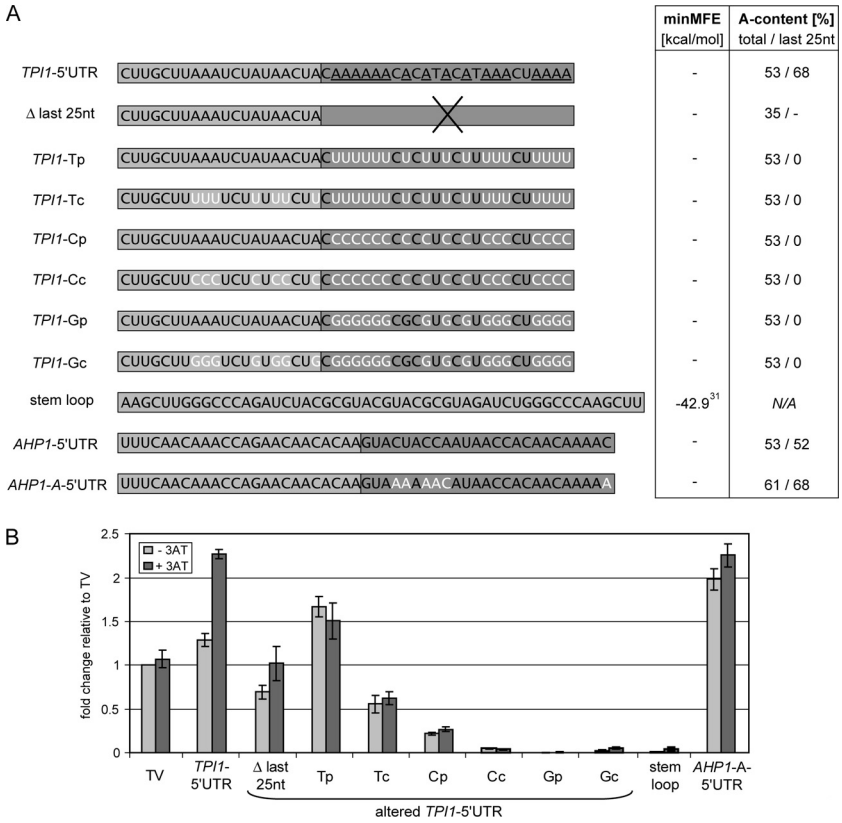

FIG. 5. **Evaluation of artificially generated 5′UTRs.** *A*, DNA-fragments were constructed and expressed via reporter-testing system, resulting in the schematically illustrated mRNA-5′UTR sequences. The corresponding minimal free energies (MFEs) were determined with RNAFOLD. For the *TPI1*- and *AHP1*-5′UTRs the last 25 nt and altered bases are highlighted. The respective adenine-contents are displayed for full length 5′UTRs and the last 25 nt. *B*, The β-galactosidase assays display the influence on *lacZ*-expression exhibited by the respective 5′UTR inserted in the reporter-testing vector under non-starvation (-3AT) and aa-starvation conditions (+3AT). The data was normalized to the plasmid copy numbers for each construct (supplemental Fig. S5B) and are displayed relative to the testing vector without 5′UTR under the respective condition.

only 52% compared with 68% for the *TPI1*-5′UTR (Table II). The 5′UTR of *AHP1* was modified to test whether any random 5′UTR sequence with a high adenine-content proximal to the AUG start codon can convey an aa-dependent increase of *lacZ*-expression. Several bases in the last 25 nt of the *AHP1*-5′UTR sequence were exchanged for adenine bases and arranged to resemble the terminal *TPI1*-5′UTR sequence, resulting in an AUG-proximal A-content of 68% for the *AHP1-A*-5′UTR (Fig. 5*A*). The evaluation of this 5′UTR enriched in downstream adenine bases does not result in a significant increase in β-galactosidase activity under aa-starvation conditions, suggesting additional specificities within the *TPI1*-5′UTR to mediate its aa-specific regulatory function than solely its increased terminal A-content and absent secondary structure formation.

Taken together, our data indicates an up-regulation in the translational rate for the *ENO1*-, *FBA1*-, and *TPI1*-mRNAs mediated by their respective 5′UTR. For *TPI1* these effects are significant enough to induce substantial changes to the Tpi1p-pool within the cell already after a short period of elevated biosynthesis levels. The bioinformatic analysis suggests weakly folded 5′UTR sequences with an enrichment of adenine bases in proximity to the AUG initiation codon to be beneficial for translation efficiency. The analysis of artificially generated 5′UTRs demonstrates that the adenine bases in the *TPI1*-5′UTR are specifically required for elevated expression levels under aa-starvation conditions and suggests that further features might contribute to this regulatory function.

DISCUSSION

The presented proteome analysis of radioactively labeled protein extracts enables the identification of proteins, whose *de novo* biosynthesis is elevated under aa-starvation conditions. Along the same lines, Smirnova and colleagues performed polysome analyses of aa-starved yeast cells, which resulted in translation profiles disclosing mRNAs with enhanced translation efficiency upon aa-withdrawal (11). Surprisingly, no significant correlations within the identified candidates can be found when comparing both data sets. Suggested by the up-regulation of biosynthesis of several proteins involved in oxidative stress response in this study but not in the analysis by Smirnova *et al.*, these discrepancies might at least partially derive from different means of inducing aa-starvation conditions. Whereas Smirnova and colleagues completely withdrew amino acids, in this study aa-starvation was induced by 10 mM 3AT, a compound that has previously been described to additionally inhibit catalases and might thereby contribute to oxidative stress (31). Nevertheless, both studies feature the striking similarity of the translational up-regulation of many candidates that are taking part in carbohydrate metabolism and energy balance, which is speculated by Smirnova *et al.* to occur in preparation of an elevated aa-biosynthesis. Whereas Smirnova and colleagues only

identify a small number of such candidates with a converse transcriptional regulation, we observe that most of our candidates belonging to this group, show a post-transcriptional up-regulation, namely Tpi1p, Fba1p, Ald6p, Pgk1p, and Eno1p. This observation is further supported by the properties of the 5′UTRs of *ENO1*, *FBA1,* and *TPI1* in mediating elevated translation rates upon aa-starvation.

Most of the evaluated 5′UTRs in this study enhanced the *lacZ*-reporter expression and yielded weak secondary structures in the bioinformatical analysis or had no structure predicted at all like the *TPI1*-5′UTR. This is in agreement with the finding that 5′UTRs of highly abundant proteins generally possess weaker secondary structures resulting in an elevated translation initiation of their respective mRNAs (29).

In addition to the mainly weak secondary structures predicted, another striking feature of the analyzed 5′UTRs is the high content of adenine bases. The analysis of variants of the unstructured *TPI1*-5′UTR containing thymine, cytosine or guanine bases in place of adenine resulted in a reduction of β-galactosidase activity with more drastic effects for the replacement by guanine and cytosine. The strongest translational repression was obtained for the partial (last 25nt) and complete substitution with guanine bases. Such guanine-rich sequences can adopt non-canonical four-stranded secondary structures, so-called G-quadruplexes, which have been shown to reduce the translational rate when located in 5′UTR sequences (32).

In addition to the overall overrepresentation of adenine bases in the analyzed 5′UTR sequences, they are especially dominant in proximity to the mRNA-initiation codon, reaching up to 68% for the last 25 nt of the unstructured *TPI1*-5′UTR (Fig. 5*A*). The substitution of these terminal adenine bases by any other nucleotide results in a complete loss of the *TPI1*-5′UTR specific up-regulation of *lacZ*-expression under aa-starvation conditions. This effect could be mediated by the described role of unstructured A-rich tracts in serving as binding sites for the poly(A) binding protein (Pab1p). This binding is suggested to be able to substitute for cap and eIF4E in recruiting eIF4G for translation initiation, thus displaying an IRES event, as previously shown for starvation-induced invasive growth in yeast (9). In addition, particularly strong eukaryotic IRES have been linked to weak secondary structures (10) as *e.g.* present for the *TPI1*-5′UTR. Accordingly, the A-rich tract within the *TPI1*-5′UTR could act as IRES element, required to mediate enhanced translational activity upon aa-starvation conditions, when cap-dependent translation initiation is reduced. This is further supported by the positioning of the A-rich tract immediately upstream of the mRNA-initiation codon, which serves as predominant localization site for IRES elements (10).

Despite the absence of an apparent secondary structure and a high adenine content in the last 25 nt of the *FPR1*- and the *AHP1-A*-5′UTR, these sequences do not significantly induce *lacZ*-expression under aa-starvation conditions, suggesting further factors to be involved in the aa-dependent regulatory function observed for the *TPI1*-5′UTR. An indication might be given by the 5′UTRs of *ENO1*, *FBA1,* and *TPI1*, representing the three 5′UTR sequences enhancing *lacZ*-expression aa-dependently. These 5′UTRs show an increased adenine content in their last 25 nt relative to the full length sequence, amounting to at least 20% (Table II). This could not be observed for any other unstructured 5′UTR analyzed including the artificially generated *AHP1-A*-5′UTR (Fig. 5*A*). This leads to the assumption that not only the absolute amount of adenine bases in the last 25 nt is of importance for the regulatory function of a 5′UTR upon aa-starvation conditions but especially their distribution along the 5′UTR sequence is of relevance.

The testing system as it is described in this study displays a very strict screening tool. It aims to identify proteins regulated via translation solely mediated by their 5′UTR sequence. An interesting continuative approach could be to expand the current reporter-testing vector to enable the incorporation of not only the 5′UTR but also the 3′UTR of an mRNA to monitor their combined influence on *lacZ*-reporter expression. Apart from the known regulative function of 5′UTRs, roles in the regulation of translation initiation have also been described for the 3′UTR as well as for the ring formation of the mRNA. Thus, a comprehensive picture of the broad range of translational control mechanisms could be obtained by the described expansion of the testing system, because a synergy of 5′ and 3′ UTR has previously been suggested to be important for the establishment of correct translation (33–36).

Taken together, this study demonstrates a well-suited approach to identify translationally regulative 5′UTR sequences of abundant proteins. The applied combination of proteomics, transcriptomics as well as bioinformatical and molecular genetic tools enabled the identification of an A-rich tract in the downstream region of the *TPI1*-5′UTR, required to mediate aa-starvation-induced elevated expression levels. The generated reporter-testing system is not only applicable under various growth conditions but also suitable to compare the translational capabilities of different deletion mutants or strain backgrounds. It therefore opens up the possibility to gain more insight into a proteins function within the cell.

Acknowledgments—We thank Verena Pretz for her outstanding technical assistance. We thank Thomas Dever and Alan Hinnebusch for providing the anti-eIF2 antibody and Jürgen Dohmen for providing the anti-Tpi1p antibody.

* This work was supported by the Deutsche Forschungsgemeinschaft.

S This article contains supplemental Figs. S1 to S6 and Tables S1 to S3.

¶ To whom correspondence should be addressed: Georg-August Universität, Institute of Microbiology and Genetics, Department of Molecular Microbiology and Genetics, Grisebachstraβe 8, D-37077 Göttingen, Germany. Tel.: ++49-551-39-3771; Fax: ++49-551-39-3330; E-mail: gbraus@gwdg.de, ovaleri@gwdg.de

REFERENCES

1. Day, D. A., and Tuite, M. F. (1998) Post-transcriptional gene regulatory mechanisms in eukaryotes: an overview. *J. Endocrinol.* **157,** 361–371
2. Holcik, M., and Sonenberg, N. (2005) Translational control in stress and apoptosis. *Nat. Rev. Mol. Cell Biol.* **6,** 318–327
3. Gebauer, F., and Hentze, M. W. (2004) Molecular mechanisms of translational control. *Nat. Rev. Mol. Cell Biol.* **5,** 827–835
4. Hinnebusch, A. G. (2000) Mechanism and regulation of initiator methionyl tRNA binding to ribosomes, Translational Control of Gene Expression, pp. 185–243, Cold Spring Harbor Laboratory, Cold Spring Harbor, NY
5. Hinnebusch, A. G. (2005) Translational regulation of *GCN4* and the general amino acid control of yeast. *Annu. Rev. Microbiol.* **59,** 407–450
6. Hinnebusch, A. G. (1993) Gene-specific translational control of the yeast *GCN4* gene by phosphorylation of eukaryotic initiation factor 2. *Mol. Microbiol.* **10,** 215–223
7. Harding, H. P., Novoa, I., Zhang, Y., Zeng, H., Wek, R., Schapira, M., and Ron, D. (2000) Regulated translation initiation controls stress-induced gene expression in mammalian cells. *Mol. Cell* **6,** 1099–1108
8. Vattem, K. M., and Wek, R. C. (2004) Reinitiation involving upstream ORFs regulates ATF4 mRNA translation in mammalian cells. *Proc. Natl. Acad. Sci. U.S.A.* **101,** 11269–11274
9. Gilbert, W. V., Zhou, K., Butler, T. K., and Doudna, J. A. (2007) Cap-independent translation is required for starvation-induced differentiation in yeast. *Science* **317,** 1224–1227
10. Xia, X., and Holcik, M. (2009) Strong eukaryotic IRESs have weak secondary structure. *PLoS One* **4,** e4136
11. Smirnova, J. B., Selley, J. N., Sanchez-Cabo, F., Carroll, K., Eddy, A. A., McCarthy, J. E., Hubbard, S. J., Pavitt, G. D., Grant, C. M., and Ashe, M. P. (2005) Global gene expression profiling reveals widespread yet distinctive translational responses to different eukaryotic translation initiation factor 2B-targeting stress pathways. *Mol. Cell. Biol.* **25,** 9340–9349
12. Valerius, O., Kleinschmidt, M., Rachfall, N., Schulze, F., López Marín, S., Hoppert, M., Streckfuss-Bömeke, K., Fischer, C., and Braus, G. H. (2007) The *Saccharomyces* homolog of mammalian RACK1, Cpc2/Asc1p, is required for *FLO11*-dependent adhesive growth and dimorphism. *Mol. Cell Proteomics* **6,** 1968–1979
13. Janke, C., Magiera, M. M., Rathfelder, N., Taxis, C., Reber, S., Maekawa, H., Moreno-Borchart, A., Doenges, G., Schwob, E., Schiebel, E., and Knop, M. (2004) A versatile toolbox for PCR-based tagging of yeast genes: new fluorescent proteins, more markers and promoter substitution cassettes. *Yeast* **21,** 947–962
14. Ito, H., Fukuda, Y., Murata, K., and Kimura, A. (1983) Transformation of intact yeast cells treated with alkali cations. *J. Bacteriol.* **153,** 163–168
15. David, L., Huber, W., Granovskaia, M., Toedling, J., Palm, C. J., Bofkin, L., Jones, T., Davis, R. W., and Steinmetz, L. M. (2006) A high-resolution map of transcription in the yeast genome. *Proc. Natl. Acad. Sci. U.S.A.* **103,** 5320–5325
16. Hilton, J. L., Kearney, P. C., and Ames, B. N. (1965) Mode of action of the herbicide, 3-amino-1,2,4-triazole(amitrole): inhibition of an enzyme of histidine biosynthesis. *Arch Biochem. Biophys* **112,** 544–547
17. Wessel, D., and Flügge, U. I. (1984) A method for the quantitative recovery of protein in dilute solution in the presence of detergents and lipids. *Anal. Biochem.* **138,** 141–143
18. Blum, H., Eyer, H., and Gross, H. J. (1987) Improved silver staining of plant proteins, RNA and DNA in polyacrylamide gels. *Electrophoresis* **8**, 93–99
19. Shevchenko, A., Wilm, M., Vorm, O., and Mann, M. (1996) Mass spectrometric sequencing of proteins silver-stained polyacrylamide gels. *Anal. Chem.* **68,** 850–858
20. Eng, J. K., McCormack, A. L., and Yates III, J. R. (1994) An approach to correlate tandem mass spectral data of peptides with amino acid sequences in a protein database. *J. Am. Soc. Mass Spectrom.* **5**, 976–989
21. Bradford, M. M. (1976) A rapid and sensitive method for the quantitation of microgram quantities of protein utilizing the principle of protein-dye binding. *Anal. Biochem.* **72**, 248–254
22. Rose, M., and Botstein, D. (1983) Construction and use of gene fusions to lacZ (β-galactosidase) that are expressed in yeast. *Methods Enzymol.* **101**, 167–180
23. Cross, F. R., and Tinkelenberg, A. H. (1991) A potential positive feedback loop controlling *CLN1* and *CLN2* gene expression at the start of the yeast cell cycle. *Cell* **65,** 875–883
24. Hofacker, I. L., Priwitzer, B., and Stadler, P. F. (2004) Prediction of locally stable RNA secondary structures for genome-wide surveys. *Bioinformatics* **20,** 186–190
25. Clote, P., Ferré, F., Kranakis, E., and Krizanc, D. (2005) Structural RNA has lower folding energy than random RNA of the same dinucleotide frequency. *RNA* **11,** 578–591
26. Hofacker, I. L., Fontana, W., Stadler, P. F., Bonhoeffer, L. S., Tacker, M., and Schuster, P. (1995) Fast Folding and Comparison of RNA Secondary Structures. *Monatshefte f. Chem.* **125**, 167–188
27. Kleinschmidt, M., Grundmann, O., Blüthgen, N., Mösch, H. U., and Braus, G. H. (2005) Transcriptional profiling of *Saccharomyces cerevisiae* cells under adhesion-inducing conditions. *Mol. Genet. Genomics* **273,** 382–393
28. Lawless, C., Pearson, R. D., Selley, J. N., Smirnova, J. B., Grant, C. M., Ashe, M. P., Pavitt, G. D., and Hubbard, S. J. (2009) Upstream sequence elements direct post-transcriptional regulation of gene expression under stress conditions in yeast. *BMC Genomics* **10**, 7
29. Ringnér, M., and Krogh, M. (2005) Folding free energies of 5′-UTRs impact post-transcriptional regulation on a genomic scale in yeast. *PLoS Comput. Biol.* **1,** e72
30. Niepel, M., Ling, J., and Gallie, D. R. (1999) Secondary structure in the 5′-leader or 3′-untranslated region reduces protein yield but does not affect the functional interaction between the 5′-cap and the poly(A) tail. *FEBS Lett.* **462,** 79–84
31. Kowaltowski, A. J., Vercesi, A. E., Rhee, S. G., and Netto, L. E. (2000) Catalases and thioredoxin peroxidase protect *Saccharomyces cerevisiae* against Ca^{2+}-induced mitochondrial membrane permeabilization and cell death. *FEBS Lett.* **473,** 177–182
32. Kumari, S., Bugaut, A., Huppert, J. L., and Balasubramanian, S. (2007) An RNA G-quadruplex in the 5′ UTR of the *NRAS* proto-oncogene modulates translation. *Nat. Chem. Biol.* **3,** 218–221
33. Gallie, D. R. (1991) The cap and poly(A) tail function synergistically to regulate mRNA translational efficiency. *Genes Dev.* **5,** 2108–2116
34. Tarun, S. Z., Jr., and Sachs, A. B. (1995) A common function for mRNA 5′ and 3′ ends in translation initiation in yeast. *Genes Dev.* **9,** 2997–3007
35. Wells, S. E., Hillner, P. E., Vale, R. D., and Sachs, A. B. (1998) Circularization of mRNA by eukaryotic translation initiation factors. *Mol. Cell* **2,** 135–140
36. Amrani, N., Ghosh, S., Mangus, D. A., and Jacobson, A. (2008) Translation factors promote the formation of two states of the closed-loop mRNP. *Nature* **453,** 1276–1280
37. Hoffman, C. S., and Winston, F. (1987) A ten-minute DNA preparation from yeast efficiently releases autonomous plasmids for transformation of *Escherichia coli*. *Gene* **57,** 267–272
38. Livak, K. J., and Schmittgen, T. D. (2001) Analysis of relative gene expression data using real-time quantitative PCR and the $2^{-\Delta\Delta\ C}{}_T$ Method. *Methods* **25,** 402–408